Histol Histopathol (2025) 40: 1083-1093

Histology and Histopathology
From Cell Biology to Tissue Engineering

ORIGINAL ARTICLE Open Access

Fortunellin attenuates sepsis-induced acute kidney injury by inhibiting inflammation and ferroptosis via the TLR4/NF-κB pathway

Liu Tianzhi [1], Zhang Yanmin[2], Xiujuan Liu[2] and Zhigang Zuo[1]

[1]Department of Critical Care Medicine and [2]Department of Gastroenterology, the First Hospital of Qinhuangdao, Qinhuangdao, Hebei, PR China

Summary. Objective. To investigate the potential protective effect of fortunellin in sepsis-induced acute kidney injury (AKI) and its underlying mechanisms.

Methods. Lipopolysaccharide (LPS)-treated human kidney proximal tubular epithelial (HK-2) cells were used as a cell model and sepsis-induced AKI was induced by cecal ligation and puncture (CLP) surgery in mice. Cell Counting Kit-8 (CCK8) assays and flow cytometry analysis were performed to examine the viability of HK-2 cells. Enzyme-linked immunosorbent assay (ELISA) was performed to investigate the content of tumor necrosis factor-alpha (TNF-α), interleukin-6 (IL-6), and interleukin-1 beta (IL-1β) *in viv*o and *in vitro*. The levels of malondialdehyde (MDA), superoxide dismutase (SOD), glutathione (GSH), and free iron (Fe^{2+}) were measured as indicators of ferroptosis. The phosphorylation levels of Interleukin-1 Receptor-Associated Kinase 4 (p-IRAK4), p65 (p-65), and inhibitor of kappa B alpha (p-IκBα) were detected by western blot as an indication of nuclear factor kappa-B (NF-κB) pathway activation.

Results. Our cell and animal experiments revealed that fortunellin exhibits significant anti-inflammatory and cytoprotective properties. Fortunellin counteracted LPS-induced cellular damage in HK-2 cells, enhancing cell survival and suppressing the secretion of pro-inflammatory cytokines. Additionally, fortunellin demonstrated potent antioxidant effects, reducing MDA and Fe^{2+} levels while increasing SOD activity and GSH content. The protective effect of fortunellin was further corroborated in the mouse model of sepsis-induced AKI. Notably, fortunellin suppressed activation of the TLR4/NF-κB pathway in the AKI model, as evidenced by decreased levels of p-p65 and p-IκBα proteins.

Conclusion. Fortunellin ameliorates inflammation and oxidative stress in sepsis-induced AKI, possibly through the modulation of the TLR4/NF-κB pathway. These findings suggest fortunellin's potential as a therapeutic agent for sepsis-associated AKI.

Key words: Fortunellin, Sepsis-induced acute kidney injury, Inflammation, Ferroptosis, NF-κB pathway

Introduction

Sepsis is an immune complication characterized by systemic organ dysfunction (Liu et al., 2022b). Generally, sepsis causes nervous system disorders, endothelial injury, and the release of vasoactive substances. These factors lead to the production of pro-inflammatory cytokines such as interleukin (IL)-1β, IL-6, IL-8, and tumor necrosis factor-α (TNF-α), triggering inflammatory and oxidative stress (Grondman et al., 2020; He et al., 2022) . Acute Kidney Injury (AKI) is a primary complication of sepsis, affecting approximately 45-70% of sepsis patients in clinical settings (Uchino et al., 2005). The pathophysiology of AKI is complicated and involves multiple pathogenic changes, including

Abbreviations. AKI, Acute Kidney Injury; AMPK, Adenosine Monophosphate-activated Protein Kinase; BUN, Blood Urea Nitrogen; CCK-8, Cell Counting Kit-8; CLP, Cecal Ligation and Puncture; Cre, Creatinine; ELISA, Enzyme-Linked Immunosorbent Assay; Fe^{2+}, Free Iron; FBS, Fetal Bovine Serum; FSP1, Ferroptosis Suppressor Protein 1; GCH1, GTP Cyclohydrolase 1; GPX4, Glutathione Peroxidase 4; GSH, Glutathione; H&E, Hematoxylin and Eosin; HK-2, Human Kidney Proximal Tubular Epithelial; IL-1β, Interleukin-1 beta; IL-6, Interleukin-6; IRAK4, Interleukin-1 Receptor-Associated Kinase 4; LPS, Lipopolysaccharide; MDA: Malondialdehyde; MEM, Minimum Essential Medium; NF-κB, Nuclear Factor kappa-B; Nrf-2, Nuclear Factor Erythroid 2-related Factor 2; PBS, Phosphate-Buffered Saline; ROS, Reactive Oxygen Species; SOD, Superoxide Dismutase; TLR4, Toll-Like Receptor 4; TNF-α, Tumor Necrosis Factor-alpha; TUNEL, Terminal deoxynucleotidyl transferase dUTP Nick End Labeling.

Corresponding Author: Zhigang Zuo, No. 258 Wenhua Road, Haigang District, Qinhuangdao City, Hebei Province, 066099, PR China. e-mail: Zhigang0019@163.com

www.hh.um.es. DOI: 10.14670/HH-18-841

renal hypoperfusion, microvascular dysfunction, tubular cell injury, and maladaptive repair processes (Basile et al., 2012). Additionally, the inflammatory cascade initiated by sepsis can directly damage kidney tissues, while oxidative stress further exacerbates cellular injury (Almazmomi et al., 2023). The interplay between these factors can lead to a rapid decline in renal function, manifesting as decreased urine output and elevated serum creatinine levels (Makris and Spanou, 2016). Understanding these complex pathways is crucial for developing effective therapeutic strategies to prevent and treat sepsis-induced AKI.

Recent studies have identified ferroptosis, a form of iron-dependent cell death, as a detrimental factor in AKI (Lin et al., 2023; Jin et al., 2024). Ferroptosis is characterized by the accumulation of lipid peroxides and iron-dependent reactive oxygen species (ROS) production (Jiang et al., 2021). This unique modality of cell death is regulated by key pathways involving system Xc-, glutathione metabolism, iron homeostasis, as well as oxidative stress (Zeng et al., 2023) . Several defense mechanisms against ferroptosis have been elucidated, including GTP cyclohydrolase 1 (GCH1), glutathione peroxidase 4 (GPX4), and ferroptosis suppressor protein 1 (FSP1). These proteins protect cells from iron-dependent lipid peroxidation by producing lipophilic antioxidants, reducing lipid hydroperoxides, and maintaining cellular redox homeostasis (Zeng et al., 2023, Zhang et al., 2023a,b). In AKI, iron overload plays a critical role in exacerbating kidney damage through various mechanisms, including increased iron availability, the Fenton reaction, mitochondrial dysfunction, and amplification of ferroptosis (Walker and Agarwal, 2016; Scindia et al., 2019; Mo et al., 2022; Ni et al., 2022). The disruption of iron homeostasis during AKI creates an environment conducive to ferroptosis, potentially leading to widespread tubular cell death and further inflammatory responses (Scindia et al., 2019; Ni et al., 2022). Targeting iron overload and ferroptosis opens new avenues for therapeutic interventions for AKI management (Walker and Agarwal, 2016; Scindia et al., 2019; Mo et al., 2022; Ni et al., 2022).

In recent years, kumquat fruit (*Fortunella japonica* Swingle) extracts have garnered increasing attention due to their potential health benefits (Lou and Ho, 2017). Among the identified bioactive compounds, fortunellin, a type of citrus flavonoid, has been shown to exhibit anti-cancer, anti-inflammatory, and antioxidant effects (Lou et al., 2016). Fortunellin was reported to inhibit ROS production and suppress inflammation in colitis by regulating the nuclear factor kappa-B (NF-κB) signaling pathway (Xiong et al., 2018). Furthermore, in a model of diabetes-induced heart injury, fortunellin was found to suppress inflammation and oxidative stress through the adenosine monophosphate-activated protein kinase (AMPK)/nuclear factor erythroid 2-related factor 2 (Nrf-2) pathway (Zhao et al., 2017). Given its potent anti-inflammatory and antioxidant properties, fortunellin represents a promising therapeutic candidate for the treatment of sepsis-induced AKI. Natural products have been extensively studied for their ability to modulate ferroptosis (Zheng et al., 2024), however, the potential effect of fortunellin on AKI-related ferroptosis warrants further exploration. In this study, we investigated the potential protective effect of fortunellin in sepsis-induced AKI and its underlying mechanisms.

Materials and methods

Cell and cell culture

Human kidney proximal tubular epithelial (HK-2) cells were procured from Procell Life Science & Technology. Co., Ltd. (Procell, Wuhan, Chian, Cat# CL-0109). The cells were cultivated in Minimum Essential Medium (MEM) supplemented with 10% fetal bovine serum (FBS) (both from Gibco, Thermo Fisher Scientific, Waltham, MA, USA) at 37°C in a 5% CO_2 incubator. Regarding cell treatments: the control group received no treatment; in the lipopolysaccharide (LPS) group, cells were incubated with 10 ng/mL LPS (Sigma-Aldrich, St. Louis, MO, USA, Cat# L2630) for 24 hours; in the LPS + fortunellin groups, culture medium containing 20/40/80 μM fortunellin (MedChemExpress, Shanghai, China, Cat# HY-119678, Purity: 95.93%) was added to the cells for 3 hours, then 10 ng/mL LPS was added and incubated for another 24 hours (Sun et al., 2021).

Cell viability assay

HK-2 cells were seeded in 96-well plates at a density of 6000 cells per well and allowed to adhere for 24 hours. Cells were then treated as described above for 24 hours. Next, 10 μL of Cell Counting Kit-8 (CCK-8) reagent (Dojindo Molecular Technologies, Kumamoto, Japan, Cat# CK04) was added to each well and incubated for 3 hours at 37°C. The absorbance was measured at 450 nm using a BioTek Synergy HTX microplate reader (BioTek Instruments, Winooski, VT, USA). Cell viability was calculated as a percentage, with the untreated group set as 100%.

Enzyme-linked immunosorbent assay (ELISA) and detection of oxidative stress

ELISA analysis and detection of oxidative stress indicators were conducted in 10 mg of tissue or $1x10^6$ HK2 cells in each experimental group. A colorimetric iron assay kit (Abcam, Cambridge, UK, Cat# ab83366) was used for intracellular free iron detection. The detection of malondialdehyde (MDA, Cat# E-EL-0060) and glutathione (GSH, Cat# E-EL-0026) was conducted using the corresponding commercial kits (Elabscience Biotechnology Co., Ltd., Wuhan, Hubei, China) according to the manufacturer's instructions. For human samples, superoxide dismutase 1 (SOD1, Elabscience

Biotechnology Co., Ltd., Cat# E-EL-H1113), TNF-α (Cat# E-EL-H0109), interleukin-6 (IL-6, Cat# E-EL-H6156), and interleukin-1 beta (IL-1β, Cat# E-EL-H0149) were measured. For mouse samples, SOD1 (Cat# E-EL-M2398), TNF-α (Cat# E-EL-M3063), IL-6 (Cat# E-EL-M0044), and IL-1β (Cat# E-EL-M0037) were measured. The relative levels of each molecule were normalized against the protein contents in each sample, which was determined using a Bradford protein assay kit (Beyotime Biotech, Beijing, China, Cat# P0006).

Flow cytometry analysis of cell death

HK-2 cells (1×10^6) were harvested and washed twice with cold PBS. Cell death was assessed using the Annexin V-FITC Apoptosis Detection Kit (BD Biosciences, San Jose, CA, USA, Cat# 556547) according to the manufacturer's instructions. Briefly, cells were resuspended in 200 μL of 1X binding buffer, then incubated with 5 μL of FITC-conjugated Annexin V and 5 μL of Propidium Iodide (PI) for 15 minutes at room temperature in the dark. After incubation, 400 μL of 1X binding buffer was added to each sample. The stained cells were analyzed using a BD FACSCanto II flow cytometer (BD Biosciences, San Jose, CA, USA).

Western blot

Cells ($1x10^6$) or tissues (10 mg) were lysed in RIPA buffer containing protease inhibitors (Thermo Fisher Scientific, Cat# 89900). Protein concentrations were determined using a BCA Protein Assay Kit (Thermo Fisher Scientific, Cat# 23225). Equal amounts of protein were separated by SDS-PAGE and transferred onto PVDF membranes (Millipore, Burlington, MA, USA, Cat# IPVH00010). Membranes were blocked with 5% bovine serum albumin (BSA) (Sigma-Aldrich, Cat# A2153) for 1h and then incubated with primary antibodies at 4°C overnight. The following primary antibodies were used (all from Cell Signaling Technology, Danvers, MA, USA, 1:1000 dilution): phospho-p65 (Cat# 3033), phospho-IκBα (Cat# 2859), total p65 (Cat# 8242), total IκBα (Cat# 4814), IRAK4 (Cat# 4363), Phospho-IRAK4 (Cat# 11927), and GAPDH (Cat# 5174). Membranes were then incubated with HRP-conjugated secondary antibodies (anti-mouse or anti-rabbit, 1:5000, Cell Signaling Technology, Cat# 7076 and 7074) for 1h at room temperature. Protein bands were visualized using a ChemiDoc Touch Imaging System (Bio-Rad Laboratories, Hercules, CA, USA) and quantified using ImageJ software (National Institutes of Health, Bethesda, MD, USA).

Animal experiments

The sepsis model in mice was established by cecal ligation and puncture (CLP) surgery as previously described (Xu et al., 2023; Guo et al., 2024). Male C57BL/6 mice (8 weeks old, 20-25 g) were obtained from the Shanghai Laboratory Animal Center (Shanghai, China). Mice were randomly divided into four groups (n=6 per group): sham, sham+fortunellin, CLP model, and CLP model+fortunellin. For the CLP procedure, the abdominal skin and muscle were incised, the cecum was ligated and punctured, and then the abdominal muscle and skin were sutured. Sham-operated mice underwent the same procedure without ligation and puncture of the cecum. Fortunellin (MedChemExpress, Shanghai, China, Cat# HY-119678) was administered at a dose of 30 mg/kg/day by oral gavage. The sham+fortunellin and CLP model+fortunellin groups received daily fortunellin treatment, while the sham and CLP model groups received an equivalent volume of vehicle (saline). Drug intervention continued for 3 weeks. At the end of the three-week treatment, all mice were sacrificed by cervical dislocation. Blood and kidney tissues were collected for further analysis. All animal experiments were approved by the Animal Care and Use Committee of the First Hospital of Qinhuangdao. All procedures were performed in accordance with the Guide for the Care and Use of Laboratory Animals published by the National Institutes of Health.

Hematoxylin and Eosin (H&E) Staining

Kidney tissues were fixed in 10% neutral buffered formalin (Sigma-Aldrich, St. Louis, MO, USA, Cat# HT501128) for 24 hours, dehydrated through a graded ethanol series, cleared in xylene, and embedded in paraffin. Sections (5-μm thick) were cut using a microtome (Leica Biosystems, Wetzlar, Germany, Model RM2245). The sections were deparaffinized in xylene, rehydrated through a graded ethanol series, and stained with hematoxylin solution (Sigma-Aldrich, Cat# MHS16) for 5 minutes. After rinsing in distilled water, sections were differentiated in 1% acid alcohol (Sigma-Aldrich, Cat# A3429) for 30 seconds and blued in 0.2% ammonia water (Sigma-Aldrich, Cat# 221228). Sections were then counterstained with eosin solution (Sigma-Aldrich, Cat# HT110232) for 30 seconds, dehydrated through graded ethanol, cleared in xylene, and mounted with DPX mountant (Sigma-Aldrich, Cat# 06522). Stained sections were examined under a light microscope (Olympus BX53, Tokyo, Japan) for histopathological changes.

Terminal deoxynucleotidyl transferase dUTP Nick End Labeling (TUNEL) Assay

Apoptosis in kidney tissue sections was assessed using the In Situ Cell Death Detection Kit, Fluorescein (Roche Diagnostics, Mannheim, Germany, Cat# 11684795910) according to the manufacturer's instructions. Briefly, paraffin-embedded kidney sections (5-μm thick) were deparaffinized, rehydrated, and permeabilized with Proteinase K (20 μg/mL in 10 mM Tris-HCl, pH 7.4) (Sigma-Aldrich, Cat# P2308) for 30

minutes at 37°C. After washing with phosphate-buffered saline (PBS), sections were incubated with the TUNEL reaction mixture for 60 minutes at 37°C in a humidified chamber in the dark. Sections were then rinsed with PBS and counterstained with 4',6-diamidino-2-phenylindole (DAPI) (Thermo Fisher Scientific, Waltham, MA, USA, Cat# D1306) to visualize nuclei. Slides were mounted with ProLong Gold Antifade Mountant (Thermo Fisher Scientific, Cat# P36930). TUNEL-positive cells were visualized using a fluorescence microscope (Olympus BX53, Tokyo, Japan) with appropriate filters. The percentage of TUNEL-positive cells was calculated by counting the number of TUNEL-positive cells divided by the total number of DAPI-stained cells in at least five random fields per section.

Data analysis

Cell experiments were repeated three times independently and data are presented as mean ± standard deviation (SD). Statistical analysis was performed using GraphPad Prism 8.0 (GraphPad Software, San Diego, CA, USA) and Student's t-test or two-way ANOVA. *p*-values <0.05 were considered statistically significant for all tests.

Results

Fortunellin attenuates LPS-induced cell death in HK-2

Fortunellin is a well-characterized bioactive chemical isolated from kumquat fruit (*Fortunella japonica* Swingle) (Fig. 1A). In this study, we first assessed the potential cytotoxicity of fortunellin in HK-2 cells. Various concentrations of fortunellin (0, 20, 40, 80 μM) were applied for 24 hours, and no significant effect on cell viability was observed in HK-2 cells (Fig. 1B). Next, the potential effect of fortunellin against LPS-

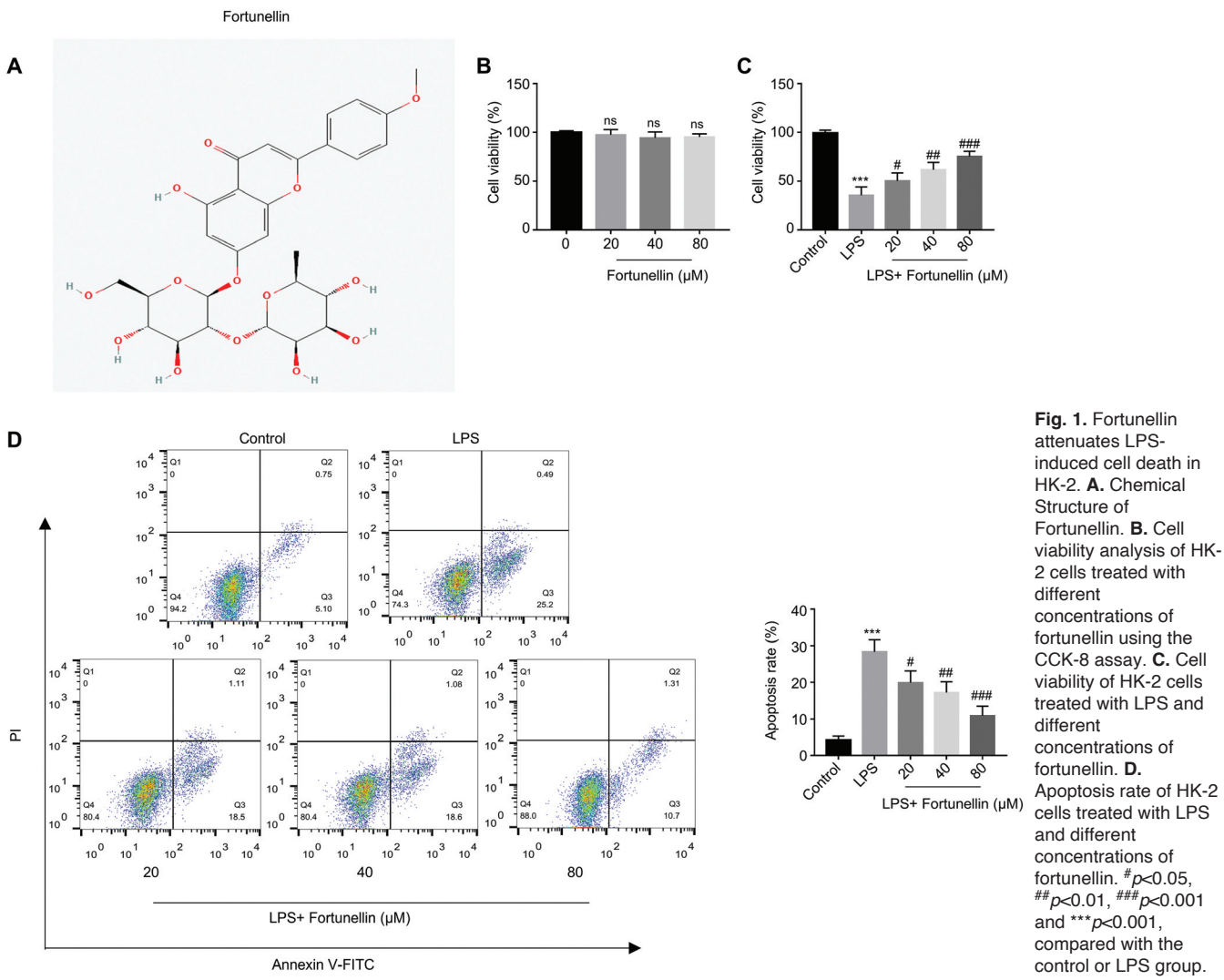

Fig. 1. Fortunellin attenuates LPS-induced cell death in HK-2. **A.** Chemical Structure of Fortunellin. **B.** Cell viability analysis of HK-2 cells treated with different concentrations of fortunellin using the CCK-8 assay. **C.** Cell viability of HK-2 cells treated with LPS and different concentrations of fortunellin. **D.** Apoptosis rate of HK-2 cells treated with LPS and different concentrations of fortunellin. $^{\#}p<0.05$, $^{\#\#}p<0.01$, $^{\#\#\#}p<0.001$ and $^{***}p<0.001$, compared with the control or LPS group.

induced injury was examined in HK-2 cells. As shown in Figure 1C, LPS treatment reduced HK-2 cell viability by approximately 50%. However, fortunellin significantly increased cell viability in a dose-dependent manner, with the highest concentration restoring cell survival to about 80% of the control group. Furthermore, LPS-induced apoptosis was also dose-dependently curtailed by fortunellin (Fig. 1D).

Fortunellin mitigates LPS-induced inflammation and ferroptosis in HK-2 cells

Given that sepsis-induced AKI is a complex syndrome involving the interplay of inflammation, oxidative stress, and ferroptosis (Walker and Agarwal, 2016; Scindia et al., 2019; Mo et al., 2022; Ni et al., 2022), we investigated the effect of fortunellin on LPS-induced inflammatory cytokine production, oxidative stress, and iron status. As shown in Figure 2A-C, LPS incubation significantly increased the levels of IL-1β, IL-6, and TNF-α compared with untreated control cells. Conversely, fortunellin reduced the secretion of these inflammatory cytokines in a dose-dependent manner.

Recent studies have identified ferroptosis as a form of programmed cell death characterized by iron overload, ROS accumulation, and GSH depletion (Scindia et al., 2019; Chen et al., 2023). Measurements of intracellular free iron ions revealed that fortunellin inhibited the LPS-stimulated increase in iron levels, with the most pronounced effect observed at 80 μM (Fig. 2D). Furthermore, fortunellin mitigated the LPS-induced increase in MDA (the byproduct of lipid peroxidation) levels (Fig. 2E), while enhancing SOD activity (Fig. 2F) and GSH content in a dose-dependent manner (Fig. 2G). These findings collectively demonstrate that fortunellin attenuates LPS-induced inflammation and ferroptosis in HK-2 cells, suggesting its potential protective role in sepsis-induced AKI.

Fortunellin suppresses LPS-induced activation of the TLR4/NF-κB pathway

To elucidate the molecular mechanisms underlying the anti-inflammatory and anti-ferroptotic effects of

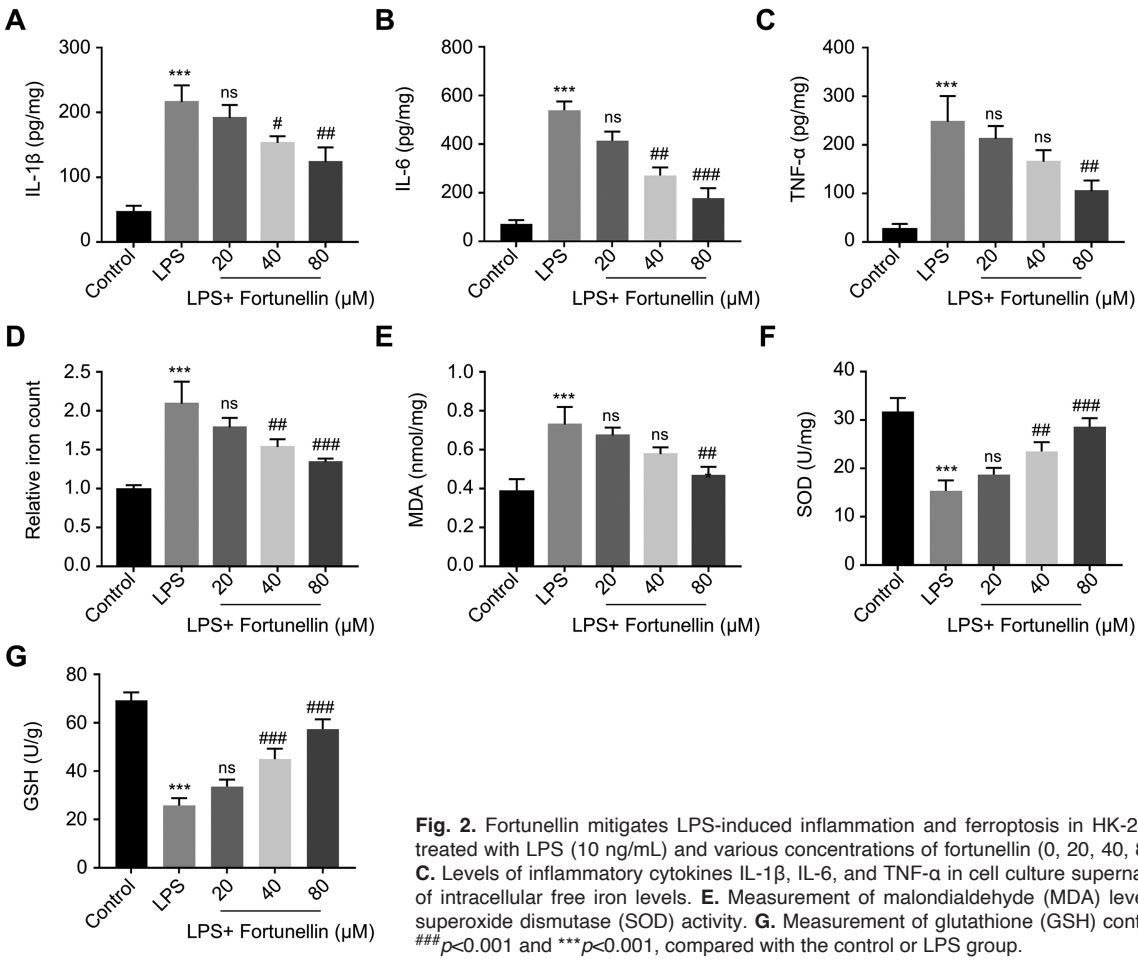

Fig. 2. Fortunellin mitigates LPS-induced inflammation and ferroptosis in HK-2 cells. HK-2 cells were treated with LPS (10 ng/mL) and various concentrations of fortunellin (0, 20, 40, 80 μM) for 24 hours. **A-C.** Levels of inflammatory cytokines IL-1β, IL-6, and TNF-α in cell culture supernatants. D. Measurement of intracellular free iron levels. **E.** Measurement of malondialdehyde (MDA) levels. **F.** Measurement of superoxide dismutase (SOD) activity. **G.** Measurement of glutathione (GSH) content. $^{\#}p<0.05$, $^{\#\#}p<0.01$, $^{\#\#\#}p<0.001$ and $^{***}p<0.001$, compared with the control or LPS group.

fortunellin, we investigated its impact on the TLR4/NF-κB signaling pathway, a well-established regulator of inflammatory responses (Liu et al., 2017). The results shown in Figure 3 demonstrate that the phosphorylation levels of IRAK4 (a signaling transducer, downstream of the TLR4 receptor), IκBα (an inhibitor of the NF-κB pathway), and p65 (a key transcription factor in the NF-κB signaling cascade) were significantly elevated by LPS, while fortunellin at 80 μM reversed the changes in p-IRAK4, p-p65, and p-IκBα levels compared with the LPS group.

The protective effect of fortunellin in the sepsis-induced AKI model

To validate the *in vitro* findings, we next investigated the effects of fortunellin in a mouse model of sepsis-induced AKI. We observed significantly elevated levels of blood urea nitrogen (BUN) and creatinine (Cre) in the CLP-induced model group, indicating impaired renal function. Fortunellin treatment (30 mg/kg) showed no effect on BUN and Cre levels in the sham group, while it significantly attenuated the CLP-induced increase in these markers in the CLP-model group (Fig. 4A). Histological analysis of kidney sections revealed no adverse effects of fortunellin in sham-operated mice. CLP mice exhibited an increased kidney injury score, which was partially ameliorated by fortunellin treatment (Fig. 4B). Besides, fortunellin significantly reduced CLP-induced apoptosis in the renal tissues, further supporting its protective role in sepsis-induced AKI (Fig. 4C). These *in vivo* findings align with our cellular experiments, demonstrating the protective effects of fortunellin against sepsis-induced AKI at both cellular and histological levels.

Fortunellin inhibits CLP-induced inflammation and ferroptosis through repressing TLR4/NF-κB signaling

To further investigate the mechanisms underlying the protective effects of fortunellin *in vivo*, we examined the expression of inflammatory cytokines and markers of ferroptosis in kidney tissues from CLP-induced septic mice. Fortunellin treatment significantly reduced the production of inflammatory cytokines in renal tissues of the CLP-induced AKI model group (Fig. 5A-C). Consistent with the cellular results, there was a significant increase in the free iron level in the model group, which was suppressed by fortunellin administration (Fig. 5D). Fortunellin treatment also reduced MDA levels while increasing GSH and SOD levels compared with CLP model mice (Fig. 5E-G). Notably, fortunellin administration alone did not induce any significant changes relative to the sham group. Furthermore, western blot analysis of kidney tissues revealed that CLP significantly increased the levels of phosphorylated IRAK4 (p-IRAK4), phosphorylated p65 (p-p65), and phosphorylated IκBα (p-IκBα), and fortunellin treatment effectively attenuated these changes (Figure 5H). These findings suggest that fortunellin may inhibit inflammation and ferroptosis in sepsis-induced AKI by dampening the NF-κB pathway.

Discussion

The present study demonstrates the protective effects

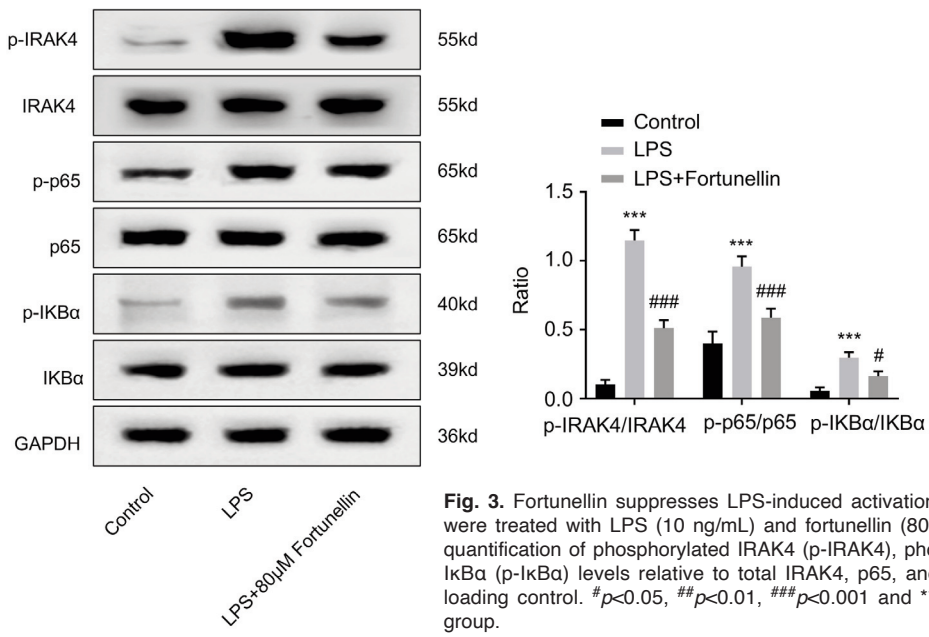

Fig. 3. Fortunellin suppresses LPS-induced activation of the NF-κB signaling pathway. HK-2 cells were treated with LPS (10 ng/mL) and fortunellin (80 μM) for 24 hours. Western blot analysis and quantification of phosphorylated IRAK4 (p-IRAK4), phosphorylated p65 (p-p65), and phosphorylated IκBα (p-IκBα) levels relative to total IRAK4, p65, and IκBα, respectively. GAPDH was used as a loading control. $^{\#}p<0.05$, $^{\#\#}p<0.01$, $^{\#\#\#}p<0.001$ and $^{***}p<0.001$, compared with the control or LPS group.

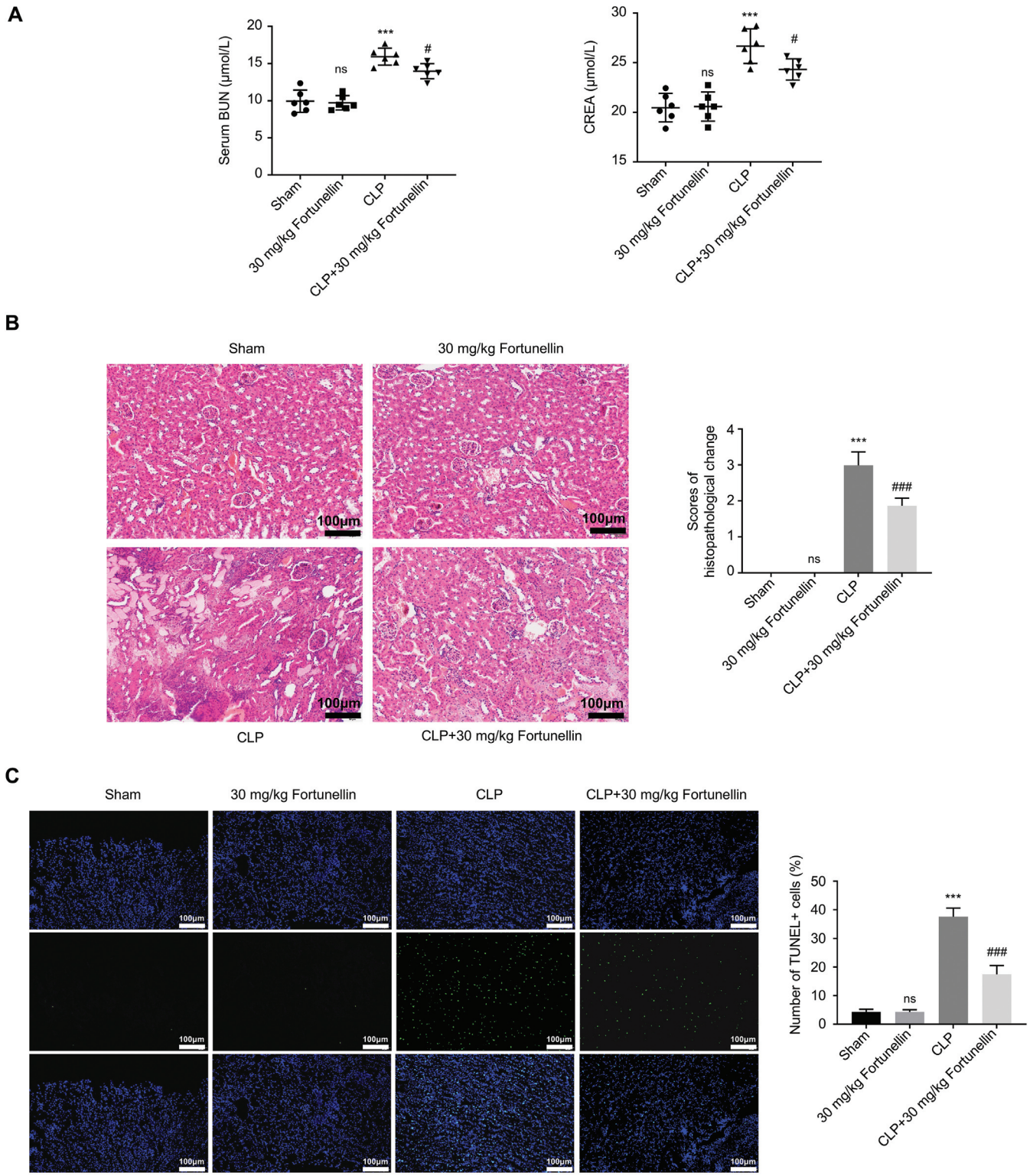

Fig. 4. The protective effect of fortunellin in the sepsis-induced AKI model. Mice were divided into four groups: sham, sham+fortunellin, CLP model, and CLP model+fortunellin. Fortunellin was administered at 30 mg/kg/day for 3 weeks. The kidney tissues and blood samples from different groups were harvested for analysis. **A.** Blood urea nitrogen (BUN) and creatinine (Cre) levels. **B.** Representative H&E staining of kidney sections and quantification of the kidney injury score. **C.** TUNEL staining of kidney sections and quantification of apoptotic cells. Scar bar=50 μm. $^{\#}p<0.05$, $^{\#\#\#}p<0.001$ and $^{***}p<0.001$, compared with the sham or CLP group.

of fortunellin against sepsis-induced AKI, both *in vitro* and *in vivo*. Our findings revealed that fortunellin significantly improved cell viability and reduced apoptosis in LPS-treated HK-2 cells. Furthermore, it attenuated LPS-induced inflammation and ferroptosis by reducing pro-inflammatory cytokine production, decreasing free iron and MDA levels, and increasing SOD activity and GSH content. Notably, fortunellin suppressed the activation of the TLR4/NF-κB pathway in these cells. In a mouse model of sepsis-induced AKI, fortunellin treatment ameliorated renal dysfunction, reduced histological damage, and decreased cell death.

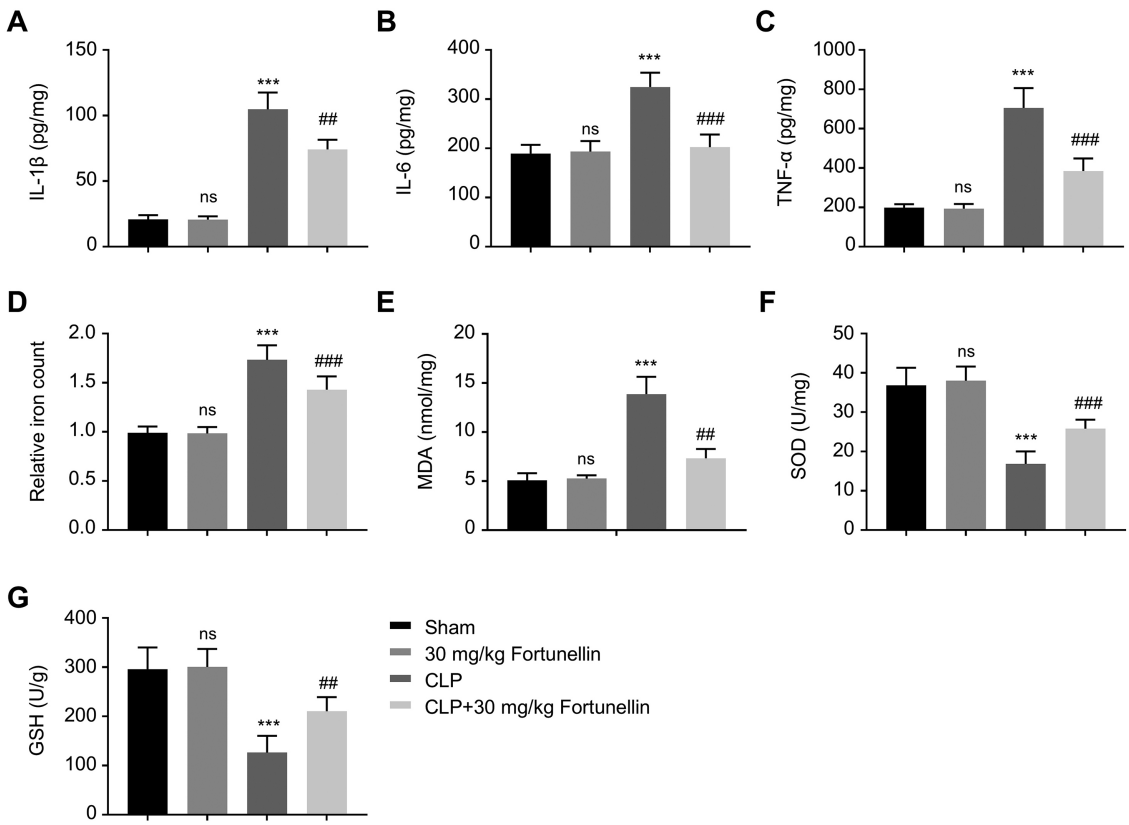

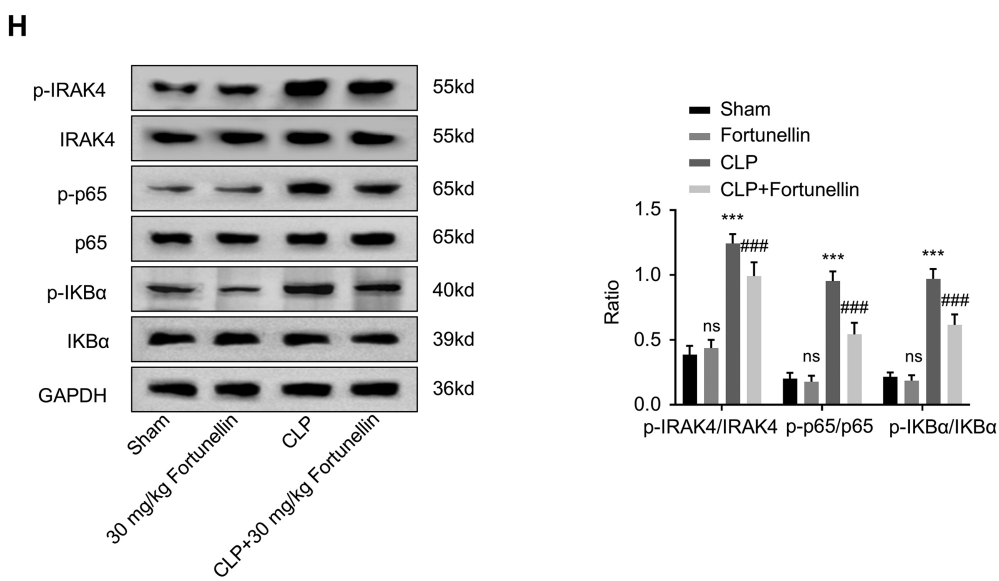

Fig. 5. Fortunellin inhibits CLP-induced inflammation and ferroptosis through repressing TLR4/NF-κB signaling. Mice were divided into four groups: sham, sham+fortunellin, CLP model, and CLP model+fortunellin. Fortunellin was administered at 30 mg/kg/day for 3 weeks. The kidney tissues from different groups were harvested for analysis. **A-C.** Levels of inflammatory cytokines IL-1β, IL-6, and TNF-α in kidney tissues. **D.** Free iron levels in kidney tissues. **E.** MDA levels in kidney tissues. **F.** SOD activity in kidney tissues. **G.** GSH content in kidney tissues. **H.** Western blot analysis and quantification of relative levels of phosphorylated IRAK4 (p-IRAK4), phosphorylated p65 (p-p65), and phosphorylated IκBα (p-IκBα) in kidney tissues. $^{\#\#}p<0.01$, $^{\#\#\#}p<0.001$ and $^{**}p<0.001$, compared with the sham or CLP group.

Consistent with the *in vitr*o results, fortunellin also inhibited inflammation and ferroptosis in vivo. These findings collectively implicate fortunellin as a potential therapeutic agent for sepsis-induced AKI, highlighting its ability to modulate multiple pathogenic processes, including inflammation, oxidative stress, and ferroptosis.

Traditional treatments for AKI often involve supportive care, including fluid management and renal replacement therapy, with limited pharmacological options (Tamargo et al., 2024). In recent years, there has been growing interest in exploring natural compounds for kidney injury treatment, given their multi-target effects and potentially lower toxicity profiles (Huang et al., 2023). Fortunellin, a citrus flavonoid glycoside, is primarily extracted from kumquat fruit (*Fortunella japonica* Swingle) using methods such as solvent extraction or ultrasound-assisted extraction (Wang et al., 2012; Lou and Ho, 2017). The anti-inflammatory and antioxidant properties of fortunellin have been widely reported in various disease models. For instance, in a study on colitis, fortunellin was found to inhibit ROS production and suppress inflammation by regulating the NF-κB signaling pathway (Xiong et al., 2018). This aligns with our findings in sepsis-induced AKI, where fortunellin effectively reduced the activation of the TLR4/NF-κB pathway. In a model of diabetes-induced heart injury, fortunellin suppressed inflammation and oxidative stress through the AMPK/Nrf-2 pathway (Zhao et al., 2017) . This effect on oxidative stress is also consistent with our observations that fortunellin treatment decreased MDA levels and increased SOD activity and GSH content in both cell and animal models of sepsis-induced AKI. Furthermore, fortunellin has demonstrated protective effects in various other inflammatory conditions, including acute lung injury (Liu et al., 2024), osteoarthritis (Upadhyay et al., 2023), and COVID-19-related inflammation (Agrawal et al., 2022), by modulating inflammatory cytokine production and oxidative stress markers. Our study extends these findings to sepsis-induced AKI, demonstrating fortunellin's ability to mitigate both inflammation and oxidative stress in this context.

Notably, our research also revealed a novel effect of fortunellin on ferroptosis, a recently recognized form of regulated cell death implicated in AKI pathogenesis (Walker and Agarwal, 2016; Scindia et al., 2019; Mo et al., 2022; Ni et al., 2022). Ferroptosis is distinct from other programmed cell death modes such as apoptosis, necroptosis, autophagy, and pyroptosis (Dixon et al., 2012; Galluzzi et al., 2018). Recent studies have established a close relationship between ferroptosis and sepsis, with evidence of its occurrence in sepsis-associated acute lung injury, cardiac injury, and renal injury (Li et al., 2022; Liang et al., 2022; Liu et al., 2022a,b; Xi et al., 2022; Zhang et al., 2023a,b). In sepsis-induced cells, ferroptosis can be triggered by the accumulation of ROS, leading to an imbalance in ROS homeostasis. This imbalance results in GSH depletion, lipid peroxidation, and impaired iron metabolism (Zheng et al., 2024). Accumulating evidence has shown that ferroptosis inhibitors, such as ferrostatin-1, can exert protective effects against septic injury in cardiac and renal tissues (Li et al., 2020). Our work demonstrated that sepsis-induced cell death exhibits ferroptotic features, which could be counteracted by fortunellin treatment. Fortunellin suppressed an increase in MDA and free iron levels, and augmented the antioxidant capacity by enhancing SOD and GSH levels in both cell and animal models of sepsis. These findings support the notion that fortunellin improves AKI by attenuating ferroptosis. However, whether fortunellin impacts different ferroptosis regulators, such as GPX4, FSP1, and GCH1, warrants further investigation.

The TLR4/NF-κB signaling pathway is a canonical pro-inflammatory pathway that can be activated by various factors (Lawrence, 2009). Activation of the TLR4 receptor leads to the recruitment of adaptor MyD88 and the activation of IRAK4 kinase, which subsequently phosphorylates the IκB kinase complex. IκB kinase phosphorylates IκB to promote its degradation, releasing the inhibition on NF-κB transcription factors, such as p65. Among the typical IκB proteins (IκBα, IκBβ, and IκBε), IκBα phosphorylation is commonly used to indicate NF-κB activation (Guo et al., 2024). NF-κB signaling has been reported to play a crucial role in kidney injury (Song et al., 2019). In our study, we showed that the inhibition of the TLR4/NF-κB pathway by fortunellin possibly contributes to its anti-inflammatory and antioxidant effects in sepsis-induced AKI, which further highlights the implication of the TLR4/NF-κB pathway in kidney injury.

Interestingly, recent studies have revealed a complex interplay between NF-κB signaling, iron overload, and ferroptosis in various pathological conditions, including AKI (Zhao et al., 2020; Chen et al., 2023). NF-κB activation can modulate iron homeostasis by regulating the expression of iron-related genes, potentially exacerbating iron overload and ferroptosis (Salama et al., 2022). Conversely, iron overload and ferroptosis can further activate inflammatory pathways, including NF-κB, creating a detrimental feedback loop (Li et al., 2022). Our findings suggest that fortunellin's ability to inhibit both the TLR4/NF-κB pathway and ferroptosis may provide a dual protective mechanism against sepsis-induced AKI. By simultaneously targeting inflammation and iron-dependent cell death, fortunellin addresses multiple detrimental conditions in AKI pathogenesis. Together, our findings underscore the potential of fortunellin as a promising therapeutic agent for sepsis-induced AKI.

Conclusion

In summary, our study demonstrates the protective effect of fortunellin on sepsis-induced AKI by attenuating inflammation, oxidative stress, and ferroptosis. The mechanism of action may involve the inhibition of the TLR4/NF-κB signaling pathway.

Fortunellin treatment was able to decrease free iron levels and lipid peroxidation while enhancing antioxidant defenses in both *in vitro* and *in vivo* models, highlighting its potential as an anti-ferroptotic agent. Further research is warranted to elucidate the detailed molecular mechanisms and assess the long-term safety and effect of fortunellin in animal models.

Ethics approval of animal work. The animal experiments were conducted in strict accordance with the guidelines of Institutional Animal Care and Use, and the animal protocols were approved by the Animal Care and Use Committee of the First Hospital of Qinhuangdao.

Availability of data and materials. The data generated and analyzed during the current study are available from the corresponding author upon reasonable request.

Disclosure of conflict of interest. The authors declared that there was no conflict of interest associated with the manuscript.

Funding statement. The study was funded by Qinhuangdao science and technology research and development program (202301A250) and Hebei Province Central Guidance Local Science and Technology Development Fund Project (246Z7736G).

References

Agrawal S., Pathak E., Mishra R., Mishra V., Parveen A., Mishra S. K., Byadgi P.S., Dubey S. K., Chaudhary A.K., Singh V., Chaurasia R.N. and Atri N. (2022). Computational exploration of the dual role of the phytochemical fortunellin: Antiviral activities against SARS-CoV-2 and immunomodulatory abilities against the host. Comput. Biol. Med. 149, 106049.

Almazmomi M.A., Esmat A. and Naeem A. (2023). Acute kidney injury: Definition, management, and promising therapeutic Target. Cureus 15, e51228.

Basile D.P., Anderson M.D. and Sutton T.A. (2012). Pathophysiology of acute kidney injury. Compr. Physiol. 2, 1303-1353

Chen Z., Wang W., Abdul Razak S.R., Han T., Ahmad N.H. and Li X. (2023). Ferroptosis as a potential target for cancer therapy. Cell Death Dis. 14, 460.

Dixon S.J., Lemberg K.M., Lamprecht M.R., Skouta R., Zaitsev E.M., Gleason C.E., Patel D.N., Bauer A. J., Cantley A.M., Yang W.S., Morrison B., 3rd. and Stockwell B.R. (2012). Ferroptosis: an iron-dependent form of nonapoptotic cell death. Cell 149, 1060-1072.

Galluzzi L., Vitale I., Aaronson S.A., Abrams J.M., Adam D., Agostinis P., Alnemri E.S., Altucci L., Amelio I., Andrews D.W., Annicchiarico-Petruzzelli M., Antonov A.V., Arama E., Baehrecke E.H., Barlev N.A., Bazan N.G., Bernassola F., Bertrand M.J.M., Bianchi K., Blagosklonny M.V., Blomgren K., Borner C., Boya P., Brenner C., Campanella M., Candi E., Carmona-Gutierrez D., Cecconi F., Chan F.K., Chandel N.S., Cheng E.H., Chipuk J.E., Cidlowski J.A., Ciechanover A., Cohen G.M., Conrad M., Cubillos-Ruiz J.R., Czabotar P.E., D'angiolella V., Dawson T.M., Dawson V.L., De Laurenzi V., De Maria R., Debatin K.M., Deberardinis R.J., Deshmukh M., Di Daniele N., Di Virgilio F., Dixit V.M., Dixon S.J., Duckett C.S., Dynlacht B.D., El-Deiry W.S., Elrod J.W., Fimia G.M., Fulda S., Garcia-Saez A.J., Garg A.D., Garrido C., Gavathiotis E., Golstein P., Gottlieb E., Green D.R., Greene L. A., Gronemeyer H., Gross A., Hajnoczky G., Hardwick J.M., Harris I.S., Hengartner M.O., Hetz C., Ichijo H., Jaattela M., Joseph B., Jost P. J., Juin P. P., Kaiser W.J., Karin M., Kaufmann T., Kepp O., Kimchi A., Kitsis R.N., Klionsky D.J., Knight R.A., Kumar S., Lee S.W., Lemasters J.J., Levine B., Linkermann A., Lipton S.A., Lockshin R.A., Lopez-Otin C., Lowe S.W., Luedde T., Lugli E., Macfarlane M., Madeo F., Malewicz M., Malorni W., Manic G., Marine J.C., Martin S.J., Martinou J.C., Medema J.P., Mehlen P., Meier P., Melino S., Miao E.A., Molkentin J.D., Moll U.M., Munoz-Pinedo C., Nagata S., Nunez G., Oberst A., Oren M., Overholtzer M., Pagano M., Panaretakis T., Pasparakis M., Penninger J.M., Pereira D.M., Pervaiz S., Peter M.E., Piacentini M., Pinton P., Prehn J.H.M., Puthalakath H., Rabinovich G.A., Rehm M., Rizzuto R., Rodrigues C.M.P., Rubinsztein D.C., Rudel T., Ryan K.M., Sayan E., Scorrano L., Shao F., Shi Y., Silke J., Simon H.U., Sistigu A., Stockwell B.R., Strasser A., Szabadkai G., Tait S. W.G., Tang D., Tavernarakis N., Thorburn A., Tsujimoto Y., Turk B., Vanden Berghe T., Vandenabeele P., Vander Heiden M.G., Villunger A., Virgin H.W., Vousden K.H., Vucic D., Wagner E.F., Walczak H., Wallach D., Wang Y., Wells J.A., Wood W., Yuan J., Zakeri Z., Zhivotovsky B., Zitvogel L., Melino G. and Kroemer G. (2018). Molecular mechanisms of cell death: recommendations of the Nomenclature Committee on Cell Death 2018. Cell Death Differ. 25, 486-541.

Grondman I., Pirvu A., Riza A., Ioana M. and Netea M.G. (2020). Biomarkers of inflammation and the etiology of sepsis. Biochem. Soc. Trans. 48, 1-14.

Guo Q., Jin Y., Chen X., Ye X., Shen X., Lin M., Zeng C., Zhou T. and Zhang J. (2024). NF-κB in biology and targeted therapy: new insights and translational implications. Signal Transduct. Target Ther. 9, 53.

He F.F., Wang Y.M., Chen Y.Y., Huang W., Li Z.Q. and Zhang C. (2022). Sepsis-induced AKI: From pathogenesis to therapeutic approaches. Front. Pharmacol. 13, 981578.

Huang J., Liang Y. and Zhou L. (2023). Natural products for kidney disease treatment: Focus on targeting mitochondrial dysfunction. Front. Pharmacol. 14, 1142001

Jiang X., Stockwell B.R. and Conrad M. (2021). Ferroptosis: mechanisms, biology and role in disease. Nat. Rev. Mol. Cell Biol. 22, 266-282.

Jin S., Liu P.S., Zheng D. and Xie X. (2024). The interplay of miRNAs and ferroptosis in diseases related to iron overload. Apoptosis 29, 45-65.

Lawrence T. (2009). The nuclear factor NF-kappaB pathway in inflammation. Cold Spring Harb. Perspect. Biol. 1, a001651.

Li N., Wang W., Zhou H., Wu Q., Duan M., Liu C., Wu H., Deng W., Shen D. and Tang Q. (2020). Ferritinophagy-mediated ferroptosis is involved in sepsis-induced cardiac injury. Free Radic. Biol. Med. 160, 303-318.

Li J., Li M., Li L., Ma J., Yao C. and Yao S. (2022). Hydrogen sulfide attenuates ferroptosis and stimulates autophagy by blocking mTOR signaling in sepsis-induced acute lung injury. Mol Immunol. 141, 318-327.

Liang N.N., Zhao Y., Guo Y.Y., Zhang Z.H., Gao L., Yu D.X., Xu D.X. and Xu S. (2022). Mitochondria-derived reactive oxygen species are involved in renal cell ferroptosis during lipopolysaccharide-induced acute kidney injury. Int. Immunopharmacol. 107, 108687.

Lin S., Wang J., Cao B., Huang Y., Sheng X. and Zhu Y. (2023). Cofilin-1 induces acute kidney injury via the promotion of endoplasmic reticulum stress-mediated ferroptosis. Hum. Cell 36, 1928-1937.

Liu T., Zhang L., Joo D. and Sun S.C. (2017). NF-κB signaling in

inflammation. Signal Transduct. Target Ther. 2, 17023.

Liu D., Huang S.Y., Sun J.H., Zhang H.C., Cai Q.L., Gao C., Li L., Cao J., Xu F., Zhou Y., Guan C.X., Jin S.W., Deng J., Fang X.M., Jiang J.X. and Zeng L. (2022a). Sepsis-induced immunosuppression: mechanisms, diagnosis and current treatment options. Mil. Med. Res. 9, 56.

Liu Y., Tan S., Wu Y. and Tan S. (2022b). The emerging role of ferroptosis in sepsis. DNA Cell Biol. 41, 368-380.

Liu D., Guo R., Shi B., Chen M., Weng S. and Weng J. (2024). Fortunellin ameliorates LPS-induced acute lung injury, inflammation, and collagen deposition by restraining the TLR4/NF-kappaB/NLRP3 pathway. Immun. Inflamm. Dis. 12, e1164.

Lou S.N. and Ho C.T. (2017). Phenolic compounds and biological activities of small-size citrus: Kumquat and calamondin. J. Food Drug Anal. 25, 162-175.

Lou S.N., Lai Y.C., Hsu Y.S. and Ho C.T. (2016). Phenolic content, antioxidant activity and effective compounds of kumquat extracted by different solvents. Food Chem. 197, 1-6.

Makris K. and Spanou L. (2016). Acute kidney injury: Definition, pathophysiology and clinical Phenotypes. Clin. Biochem. Rev. 37, 85-98.

Mo M., Gao Y., Deng L., Liang Y., Xia N. and Pan L. (2022). Association between iron metabolism and acute kidney injury in critically Ill patients with diabetes. Front. Endocrinol. 13, 892811.

Ni L., Yuan C. and Wu X. (2022). Targeting ferroptosis in acute kidney injury. Cell Death Dis. 13, 182.

Salama S.A., Abdel-Bakky M.S. and Mohamed A.A. (2022). Upregulation of Nrf2 signaling and suppression of ferroptosis and NF-κB pathway by leonurine attenuate iron overload-induced hepatotoxicity. Chem Biol. Interact. 356, 109875.

Scindia D.Y., Leeds J. and Swaminathan S. (2019). Iron homeostasis in healthy kidney and its role in acute kidney injury. Semin. Nephrol. 39, 76-84.

Song N., Thaiss F. and Guo L. (2019). NFκB and Kidney Injury. Front. Immunol. 10, 815.

Sun J., Wei S., Zhang Y. and Li J. (2021). Protective Eeffects of astragalus polysaccharide on sepsis-induced acute kidney injury. Anal. Cell. Pathol. 2021, 7178253.

Tamargo C., Hanouneh M. and Cervantes C.E. (2024). Treatment of acute kidney injury: A review of current approaches and emerging innovations. J. Clin. Med. 13, 2455.

Uchino S., Kellum J.A., Bellomo R., Doig G.S., Morimatsu H., Morgera S., Schetz M., Tan I., Bouman C., Macedo E., Gibney N., Tolwani A., Ronco C., Beginning and Ending Supportive Therapy for the Kidney Investigators (2005). Acute renal failure in critically ill patients: a multinational, multicenter study. JAMA 294, 813-818.

Upadhyay P., Kalra D., Nilakhe A.S., Aggrawal V. and Gupta S. (2023). Polyherbal formulation PL02 alleviates pain, inflammation, and subchondral bone deterioration in an osteoarthritis rodent model. Front. Nutr. 10, 1217051.

Walker V. J. and Agarwal A. (2016). Targeting iron homeostasis in acute kidney injury. Semin. Nephrol. 36, 62-70.

Wang Y.W., Zeng W.C., Xu P.Y., Lan Y.J., Zhu R.X., Zhong K., Huang Y.N. and Gao H. (2012). Chemical composition and antimicrobial activity of the essential oil of kumquat (Fortunella crassifolia Swingle) peel. Int. J. Mol. Sci. 13, 3382-3393.

Xiong Y., Qiu J., Li C., Qiu Y., Guo L., Liu Y., Wan J., Li Y., Wu G., Wang L., Zhou Z., Dong J., Du C., Chen D. and Guo H. (2018). Fortunellin-Induced modulation of phosphatase and tensin homolog by MicroRNA-374a decreases inflammation and maintains intestinal barrier function in colitis. Front. Immunol. 9, 83.

Xi L., Gy Z., Guo R. and N. Cui (2022). Ferroptosis in sepsis: The mechanism, the role and the therapeutic potential. Front. Immunol. 13, 956361.

Xu Z., Wang X., Kuang W., Wang S. and Zhao Y. (2023). Kaempferol improves acute kidney injury via inhibition of macrophage infiltration in septic mice. Biosci. Rep. 43, BSR20230873.

Zeng W., Long X., Liu P.S. and Xie X. (2023). The interplay of oncogenic signaling, oxidative stress and ferroptosis in cancer. Int. J. Cancer 153, 918-931.

Zhang X.D., Liu Z.Y., Wang M.S., Guo Y.X., Wang X.K., Luo K., Huang S. and Li R.F. (2023a). Mechanisms and regulations of ferroptosis. Front. Immunol. 14, 1269451.

Zhang L., Rao J., Liu X., Wang X., Wang C., Fu S. and Xiao J. (2023b). Attenuation of sepsis-induced acute kidney injury by exogenous H2S via inhibition of ferroptosis. Molecules 28, 4770.

Zhao C., Zhang Y., Liu H., Li P., Zhang H. and Cheng G. (2017). Fortunellin protects against high fructose-induced diabetic heart injury in mice by suppressing inflammation and oxidative stress via AMPK/Nrf-2 pathway regulation. Biochem. Biophys. Res. Commun. 490, 552-559.

Zhao Z., Wu J., Xu H., Zhou C., Han B., Zhu H., Hu Z., Ma Z., Ming Z., Yao Y., Zeng R. and Xu G. (2020). XJB-5-131 inhibited ferroptosis in tubular epithelial cells after ischemia-reperfusion injury. Cell Death Dis. 11, 629.

Zheng D., Jin S., Liu P.S., Ye J. and Xie X. (2024). Targeting ferroptosis by natural products in pathophysiological conditions. Arch. Toxicol. 98, 3191-3208.

Accepted October 30, 2024